

PRELIMINARY ANALYSIS OF TEMPERATURE EFFECTS AND MANEUVER-INDUCED DEFORMATIONS ON FBG OPTIC FIBER INTEGRATED SYSTEMS

Alessandro Aimasso¹, Matteo Bertone¹, Carlo Ferro¹, Matteo D.L. Dalla Vedova¹ & Paolo Maggiore¹

¹Department of Mechanical and Aerospace Engineering, Politecnico di Torino, Italy

Abstract

This article examines the data provided by a network of Fiber Bragg Grating (FBG) sensors integrated into an Unmanned Aerial Vehicle (UAV) structure. The primary objective of this study was to assess the feasibility of utilizing such sensors as a monitoring system for maneuver-induced deformations and temperature variations. The aim is to provide a tool that enhances the reliability of navigation systems. For this purpose, the FBG sensors were strategically integrated into various positions on the UAV. Specifically, they were arranged along one wing half, spanning its wingspan, and on the fuselage, positioned near its center of mass as feasible. The experimental trials were conducted in two phases, with the initial phase executed on the ground and the subsequent phase conducted in flight. The primary objective of the first phase was to ascertain the dynamic response of the structure experimentally. This aimed to assess the minimum sampling frequencies required during flight phases. During the flight test, due to limitations on the amount of data that could be transmitted to the ground, it became necessary to lower the sampling frequencies below the minimum values determined during the ground phase. Despite these limitations, the FBG-based sensors demonstrated their efficacy in capturing dynamic structural changes during maneuvers, offering valuable insights into mechanical deformation and temperature fluctuations. Comparing the results provided by the FBG network with the data supplied by a traditional accelerometer placed on the UAV throughout all phases, the proposed system presents a promising approach to provide an alternative data source, thereby enhancing the reliability of current navigation systems. This sensor network, therefore, enables the provision of a dataset originating from a distinct physical principle, consequently avoiding the same sources of disturbance and malfunction.

Keywords: Aerospace systems, Fiber Bragg Gratings, Innovative Sensors Networks, UAV

1. Introduction

The development of systems, especially in the aerospace field, of ever-increasing complexity requires the ability to leverage a large amount of information. In particular, this data (whether simple physical parameters or qualitative information defined by their combination) must increasingly be generated by sensors capable of delivering high performance even when used in particularly harsh environmental conditions. Furthermore, the growing level of technological complexity, combined with the need to ensure high standards of quality and safety, necessitates the development of "smart systems". This means to dispose a set of components capable of providing crucial real-time and autonomous information about their own operating state and/or health. It is therefore necessary to develop a vast network of sensors directly integrated into the structures under consideration or, alternatively, that can be applied with minimal invasiveness by ensuring a high level of electromagnetic compatibility. Fiber optic sensors, with their unique physical characteristics, are currently the only technology capable of simultaneously guaranteeing all these aspects [1]-[7].

The purpose of the current work is a preliminary assessment of an optical fiber sensor network performance for monitoring an aircraft, in this case, an UAV, in real-time [8]. Specifically, the feasibility of using fiber Bragg grating sensors (FBG) to monitor the operating temperature of the

entire aircraft and its parts, along with deformations resulting from wing deflection due to maneuver loads, is investigated. Collecting these data can provide crucial information about the proper functioning of all components during different flight phases and, more generally, the health status of specific components. Optical fiber makes it possible to develop the aforementioned "smart systems," capable of providing a large amount of real-time data about themselves [9]. The information is expressed in terms of physical parameters, essential for diagnostic, prognostic, and predictive maintenance activities and for assessing specific performances of the aircraft during its flight.

The choice to use optical fiber sensors is closely linked to the physical characteristics of the fiber itself [1]. It ensures minimal invasiveness during the application, allowing for its use when externally bonded to the parts to be instrumented or when directly laminated within the material or structure during its fabrication [10]. This is coupled with the ability to multiplex many sensors on the same communication line. Moreover, being a glass fiber, signal transmission is purely optical, offering significant advantages. Firstly, it is immune to electromagnetic interference and, in turn, does not generate any. Additionally, it does not require an electrical current for data transmission, avoiding the possibility of igniting fires. Finally, it ensures excellent performance in a relatively high-temperature range, suitable for both aeronautics and space applications [11], [12]

In the case study described in this work, a network of FBG sensors was deployed on a carbon fiber UAV to detect specific parameters, particularly temperature and deformation, along the wingspan and at additional strategic points corresponding to the most safety-critical components. Ultimately, due to the distributed presence of a significant number of sensors, the integrated optical sensor network is intended to serve as a tool to enhance the reliability of navigation systems. In this regard, the data collected by the sensors can be utilized to develop a control logic that provides information about the aircraft's attitude. In this way, data detected by FBG sensors could verify the reliability of attitude data measured by the onboard inertial units.



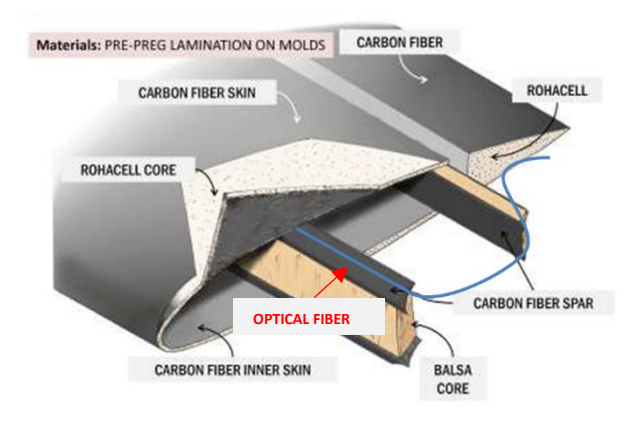


Figure 1 – The Anubi UAV (left) and a detail of the wing's structure with optical fiber (right)

2. Materials and methods

The work was carried out using an experimental setup composed of an UAV named Anubi, developed by the Icarus student team at Politecnico di Torino. It is an electrically powered model aircraft with a wingspan of 6 m and a maximum takeoff weight (MTOW) of 20kg. The UAV features a modular structure made of carbon fiber-reinforced polymer, allowing the integration of FBG sensors during the lamination of the structure's sections.

The FBG sensors, along with the data acquisition system, were thus employed for monitoring temperature and mechanical deformations. Specifically, for this initial preliminary analysis, temperature sensing was chosen for the most critical components of the propulsion system, while mechanical sensing was selected for the sensors integrated into the wing. For the development of the experimental setup, the instrumentation available at the Politecnico di Torino was used, along

with the expertise gained in using FBG sensors for measuring temperature and deformation and for integration into aerospace systems [13] - [15].

The testing campaign was divided into distinct phases. Firstly, a preliminary thermal calibration was conducted for the sensors used for the propulsion system monitoring. Subsequently, ground tests and then flight tests were carried out. The ground test initially focused on the thermal analysis of the propulsion system, particularly paying attention to the overheating of the batteries powering the electric motor. Following this, the ground tests were used to characterize the mechanical response of the sensorized semi-wing. This information was crucial for defining the requirement for the amount of data the telemetry system must be capable of transmitting to the ground station in real-time. Finally, the flight test was conducted to obtain an initial set of data provided by the optical sensors in response to the dynamic stresses typical of a structure in flight. The information measured by the optical sensors was then compared with the data collected from the inertial platform (IMU) onboard the UAV.

2.1 Optical fibers sensors and data acquisition system

A Bragg grating (FBG sensor) is a short section of optical fiber in which, through a specific laser photo-incision technique, it is possible to generate a periodic variation in the refractive index of the material. This periodic variation makes the grating a frequency-selective mirror. In other words, it reflects a specific frequency of the light spectrum that passes through it. This reflected frequency, called Bragg frequency, depends on the grating pitch. This dependency allows to associate the optical frequency variation with the variation of the physical parameter acting on the sensor itself, by the general equation:

$$\Delta \lambda = K_T \Delta T + K_{\varepsilon} \Delta \varepsilon \tag{1}$$

Thanks to the linearity of the optical response to thermal and mechanical stimuli, it is possible to transform the FBG into a sensor dedicated to a specific physical parameter (such as temperature) or to associate the optical variation induced by mechanical deformation with the broader and more complex phenomenon that generated it. The first case was applied for the thermal monitoring of the propulsion system, while the second was carried out with the sensors on the wing.

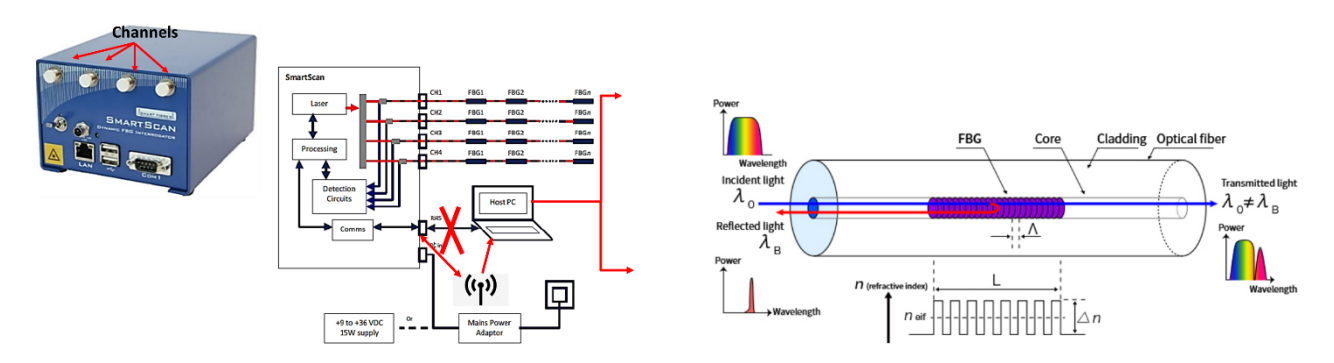


Figure 2 – The data acquisition system (left) and the working principle of FBG (right)

The data collected by the FBGs were acquired and transmitted through a telemetry and acquisition system consisting of: a *SmartScan interrogator* used to read the measurements made by the sensor network installed on the UAV; a *9V lithium-polymer (LiPo) battery* required to power the interrogator; a *Raspberry Pi* board connected to the internet via a *dongle* and, through *an Ethernet connection* with the interrogator and the use of software, was used to receive and forward the data to a cloud database; finally, a *power bank* to power the Raspberry Pi [8].

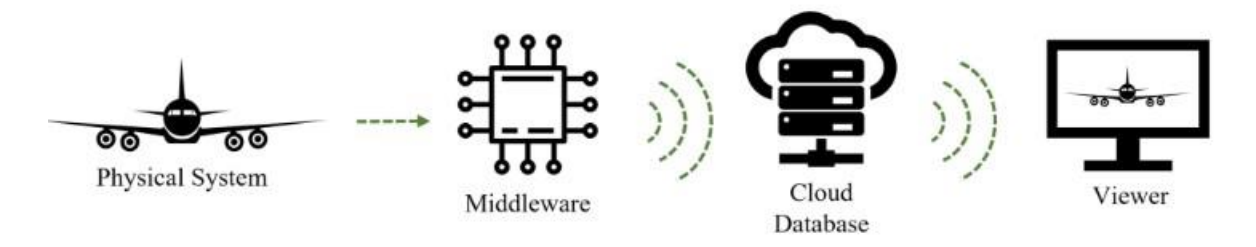


Figure 3 – Scheme of data telemetry

2.2 UAV sensorization

The FBG sensors were strategically integrated into various positions on the UAV. Specifically, they were arranged along one wing half, spanning its wingspan, and on the fuselage, positioned near its center of mass as feasible. Moreover, a fiber on the fuselage's dorsal side serves as a temperature sensor [15], and a final fiber on the landing gear assesses its behavior during the landing and liftoff phases. In addition to optical sensors, the UAV was also equipped with an Inertial Measurement Unit (IMU) and traditional sensors for measuring environmental conditions. Describing in detail the process of sensors placing on the aircraft for thermal monitoring, three sensors were placed. The first one (whose realization, calibration, and installation process is described in [15]), was positioned on the fuselage to filter the thermal contribution from the overall response provided by the sensors integrated into the wing. The other ones were specifically designed to create minimally invasive packaging that was immediately usable and allowed the FBG to be sensitive solely to thermal phenomena, thus eliminating all mechanical contributions.

The packaging was made of twin aluminum layers (3x3 cm) linked together with double-sided tape, with the latter having a square shape cut in the center where the sensor is put so that it can stretch with heat. Because of the low thermal inertia and high thermal conductivity of aluminum, this solution was considered to protect it and detect temperature in a faster and more accurate manner than a previous pipe placed on the fuselage. This packaging was stabilized with hot glue and an heat-shrinkable sheath. Once the sensor was created, it was calibrated through a series of repeated thermal cycles. This preliminary testing phase was essential not only to validate the proper functioning of the sensor but also to demonstrate that the calibration itself was independent of boundary conditions. This made the sensor sufficiently reliable as a data source for the following test campaigns.

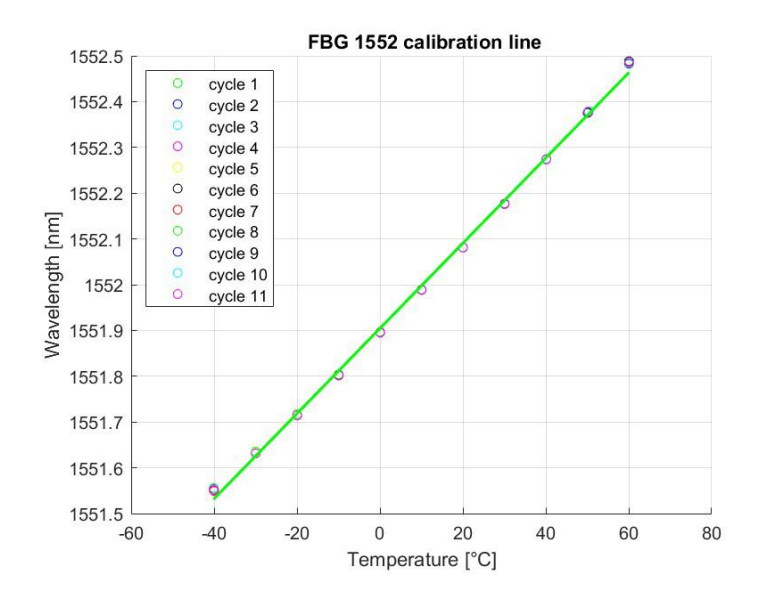


Figure 4 – FBG calibration curve

The thermal cycle technique consists of nine stages, ranging from -40 °C to 50 °C, beginning with the lowest temperature and gradually increasing to the highest, with a stable temperature lasting thirty minutes. Following the conclusion of this time frame, the next stage begins, raising the temperature by 10 °C.

The overall cycle is repeated ten times. These extremes of temperature were adjusted to not melt the adhesive and to do a sufficient number of heat tests, acquiring at 2.5 Hz; restarting, the chamber reduced its temperature to -40°C and then elevated it to 50°C.

The UAV propulsion system is essentially composed of 3 main components:

- AXI 2826/10 GOLD LINE V3 electrical motor. a brushless motor with neodymium magnets and a spinning casing, designed to transfer extremely high torque, allowing the rotation of big diameter and pitch propellers without the need for a gearbox.
- FullPower PRO, 85A SBEC Electronic Speed Control (ESC) is an electronic circuit that controls and regulates the speed of an electric motor using the current flowing through the motor windings. It may also enable motor reversal and dynamic braking.;
- WELLPOWER LIPO ULTIMA 5200 MAH/11.1 VOLT 3S 35/70C CH8 supply battery pack:
 Abbreviated as LiPo, it is a rechargeable lithium-ion battery that uses a polymer electrolyte
 rather than a liquid electrolyte to provide specific energy to the ESC. It has a higher specific
 energy than other lithium battery types and is utilized in applications where weight is an
 important factor, such as this case.

Following a preliminary analysis of the propulsion system, the power supply battery and the Electronic Speed Control (ESC) were selected for this test because they are the most thermally critical components, making it critical to validate the applicability of FBGs in terms of aerospace system diagnostics.

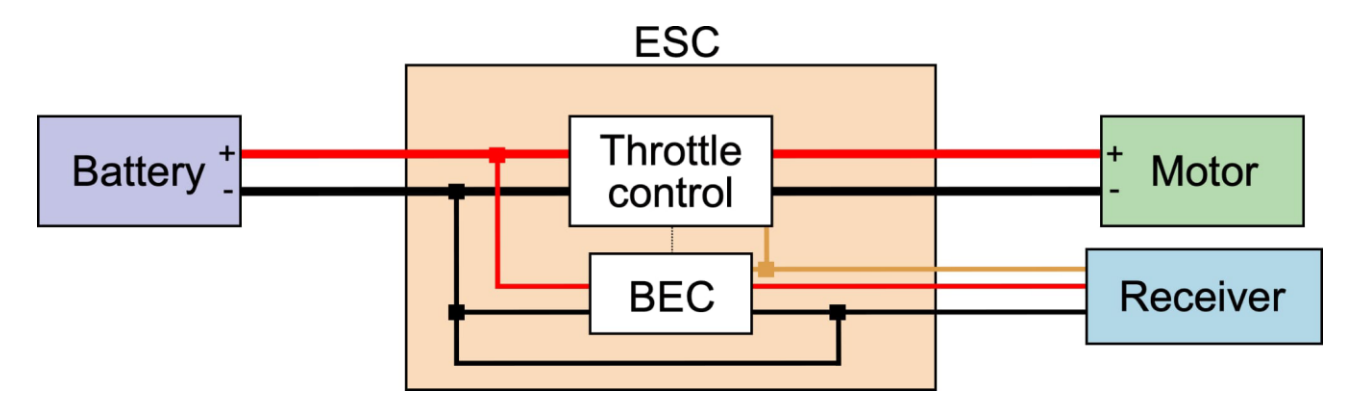


Figure 5 – UAV propulsion system scheme

The remaining FBG sensors were attached to the carbon fiber structure of the UAV. Specifically, they were positioned along the spar and subsequently covered by the wing's outer skin. Two lines of sensors were placed, one on the dorsal side and one on the ventral side, for a total of 11 sensors. These sensors are used to measure the structural deformations imposed by flight loads. Unlike the previous case, however, it was not necessary to perform a mechanical calibration process.

The desired measurement is not the precise physical strain but rather the correlation between the optical output and the overall dynamics of the aircraft. To this end, an inertial measurement unit (IMU) was also integrated on board, positioned inside the fuselage. This unit is composed of GPS (which was not used in this case), an altitude sensor, and a gyroscopic sensor, making it possible to obtain data about the linear accelerations. During test executions, both the IMU and the FBG interrogator were placed inside the fuselage, each powered by a dedicated battery.

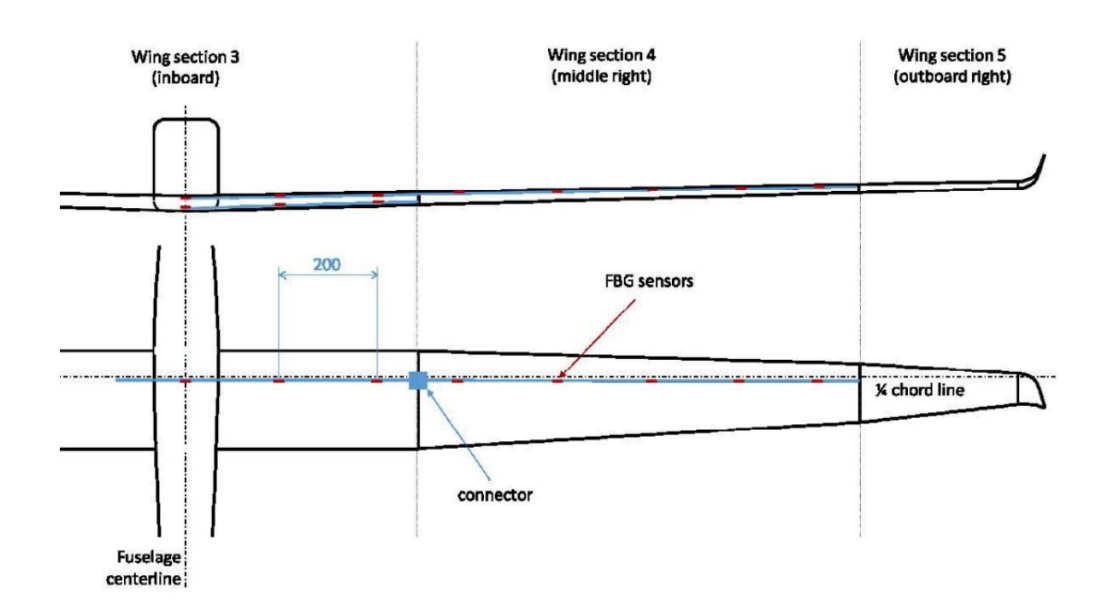


Figure 6 – Scheme of FBG placing along the wingspan

2.3 Test campaign definition

The test campaign was divided into three distinct phases:

- Thermal test of the propulsion system on the ground
- · Mechanical test of the structural response on the ground
- Flight test for validation and data transmission analysis

The thermal test campaign was conducted on the ground, with the propulsion system and flight controls activated, and the aircraft securely stationary to safely throttle the engine, simulating different flight maneuvers. One FBG sensor was placed on the surface of the battery powering the engine, while a second grating was applied to the ESC. After completing the experimental setup, the sensors were connected to the interrogator placed in the fuselage, and the test was carried out by applying different throttle levels to the engine for a period comparable to the duration of a flight. The data was acquired using the *SmartSoft* software provided by the interrogator's manufacturer, and for simplicity, the connection to the PC was made via a LAN cable.





Figure 7 – FBG on the ESC (left) and on the battery (right)

The ground test campaign was further divided into two distinct tests. The first one involved the instrumented half-wing to be stressed by progressively increasing loads, while the second simulated the instant of landing. In both cases, the physical setup included the installation of the interrogator on the fuselage, the optical fibers connected to it and the inertial platform, positioned in the compartment for the interrogator too. As in previous tests, the PC was connected to the interrogator via a LAN cable. However, this choice was not made for simplicity of acquisition, but rather to exploit the instrument's maximum acquisition frequency. Wireless data transmission does not yet guarantee equal performance, and the purpose of this ground test was to define a requirement for this parameter. Consequently, the acquisition frequency of the interrogator was set to 2500 Hz, while the IMU always acquired at 250 Hz. Data from the FBG sensors were generated using SmartSoft software and then imported into the Matlab environment, where they were saved along with the data from the inertial platform. A custom code was written to filter the data from the interrogator and make the optical output comparable to that of the IMU. Using Matlab-Simulink, the data were analyzed through FFT to identify the natural frequencies of the structure. The data provided by this analysis, therefore, represent the starting point and fundamental requirement for the telemetry system.





Figure 8 – Anubi during ground test

As the final step, a flight test was conducted. In this case, the data was acquired and transmitted to the ground wirelessly as previously described and presented. The obtained data were then compared with those saved by the inertial platform to verify the sensitivity of the FBG sensors. Additionally, the amount of information collected was compared with the requirements identified in the ground tests to evaluate the overall performance of the system and to provide any further requirements.

The analysis focused on calculating the correlation between the acceleration read along the z-axis by the inertial platform and the strain value read by the FBG sensors. In this case, the objective was to highlight the possibility of reconstructing inertial data using a network of sensors distributed and integrated into the structure itself. The potential of this approach is twofold. On one hand, it allows for redundancy of electronic information directly with information generated by a completely separate sensor system. On the other hand, it enables the use of FBG sensors for an extremely versatile and accurate loads mapping of the entire sensorized surface.

To achieve a reliable comparison, a low-pass filter was applied to the IMU results, enabling a more effective comparison between data from IMU and FBG sensors. The Pearson correlation coefficient (R) was then calculated to measure the strength of the relationship between the two variables. This method is commonly used to establish that measurements taken by conventional sensors can also be obtained using FBG sensors.

3. Results and discussion

The results obtained, although not yet final, have proven to be very interesting and extremely useful for the development of more complex, precise and effective control logics. In particular, the extreme sensitivity of the FBG gratings and the reliability of the proposed application methodology can be considered demonstrated. The results of the various tests conducted are detailed in the following subsections.

3.1 Thermal test

Thanks to the previous thermal calibration of the sensors, it was possible to instantly convert the wavelength values detected by the instrumentation into the temperature of both the battery and the ESC. Additionally, the extremely rapid response of the optical fiber allowed for precise identification of all thermal transients that the test induced on the two analyzed components. More in details, the exponential evolution of the wavelengths trends observed from FBG on both devices is characteristic of a thermal system. This observation provides an initial indication that the thermal response may be satisfactory.

During the take-off simulation phase, there is an increase in the power required by the electric motor, resulting in the heating of both the ESC and the battery. Consequently, the wavelength values increase, as evidenced by the graphs. Conversely, during the descent and landing simulation phases, a decrease in power to reduce the drone's speed brings the system in cooling of the components, as confirmed by optical data. To better understand the thermal response, the graphs depicting temperature trends measured by the FBG sensors are presented. The linear relationship between wavelength and temperature is apparent, as the trends remain consistent with the previous graphs. This consistency demonstrates the practicality of using FBG sensors for monitoring this critical physical quantity in system monitoring. The temperature trends evolve exponentially, akin to a first-order system such as a traditional temperature probe. The initial temperature of the battery increased with each test, indicating how they were conducted within a few minutes of each other, preventing the battery from cooling down fully.

Additionally, as the battery discharged, it warmed up more. The different cooling rates between the two components are attributed to their distinct thermal inertias and the significant difference in mass, as highlighted by the technical data. This disparity results in a slower cooling rate for the battery, accurately recorded by the sensor. Despite minor oscillations caused by sensor vibrations induced by airflow generated by the propeller, more pronounced in the third test due to data acquisition at 25 Hz, the long oscillations in the second test are noteworthy. Therefore, it can be concluded that these sensors exhibit a great response speed, a crucial aspect for conducting effective diagnostic analysis of components subject to heating and potential hazards. It is also important to consider that the ESC and battery are positioned on top of each other, leading to mutual heat exchange and greater oscillations, particularly in the battery's transient phase when the electric motor is switched off. Ultimately, the temperatures shown in the graphs are consistent with those reached on other occasions for both devices prior to the development of these sensors. These findings are significant for the main objective of this work, demonstrating that fiber-optic sensors offer a thermal response characterized by valuable speed, sensitivity, and accuracy. This provides a solid foundation for further future developments in aerospace applications.

Finally, the temperature sensor previously developed, tested, and validated in the laboratory by the research group has proven fully functional. Unlike its electronic counterpart, it did not experience disturbances in the presence of electromagnetic fields generated by onboard electronics. Moreover, the developed thermal sensor proved to detect the temperature in safety-critical components, such as the battery and the gearbox of the electric motor.

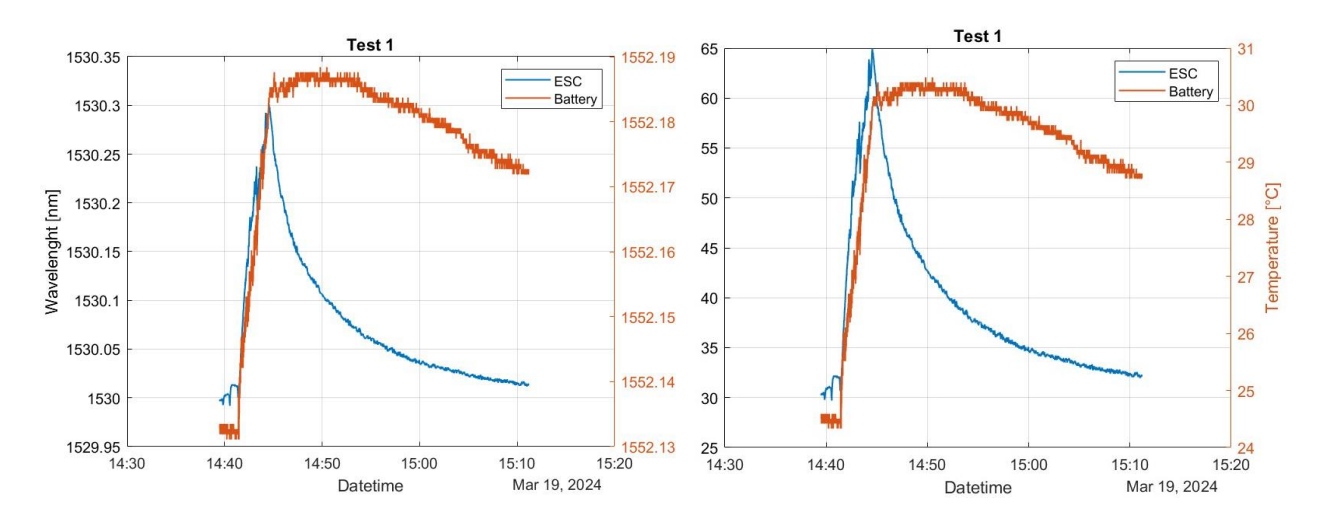


Figure 9 – FBG data expressed in wavelength (left) and converted in temperature (right)

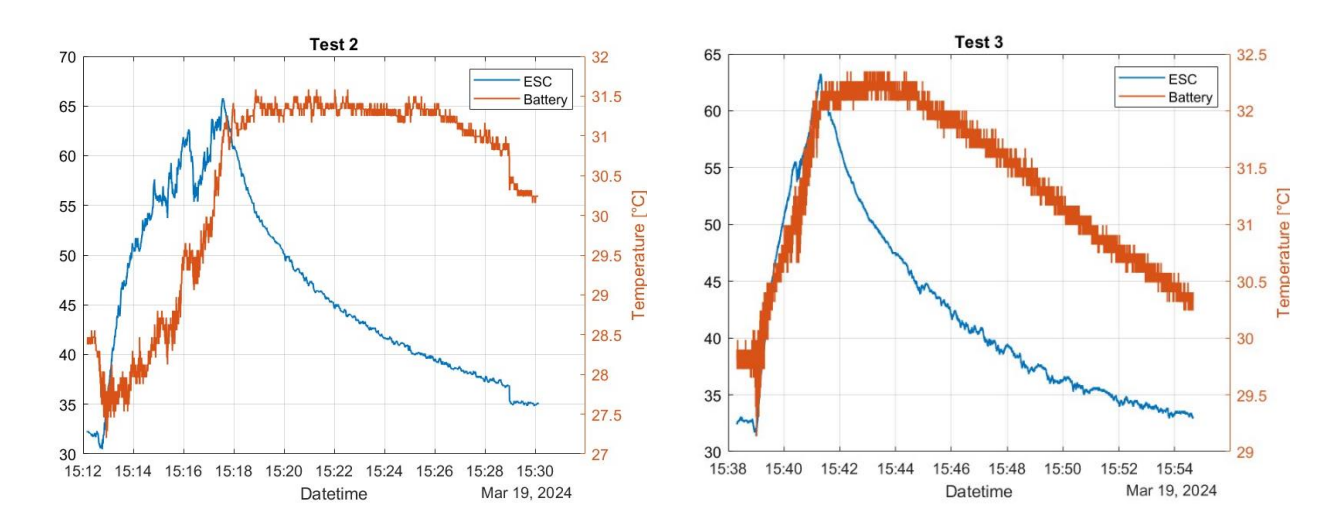


Figure 10 – Repetition of thermal test

3.2 Ground test

During the ground test phase, the structure response to impulsive loads was primarily analyzed to determine the minimum transmission frequency requirement of the telemetry system. After an FFT analysis of data from all FBGs laminated in the wing, peaks were consistently observed at approximately 2 Hz and 5 Hz. Consequently, a minimum requirement was set at least at 10 Hz. The same results were obtained for all the analyzed sensors in two test campaigns.

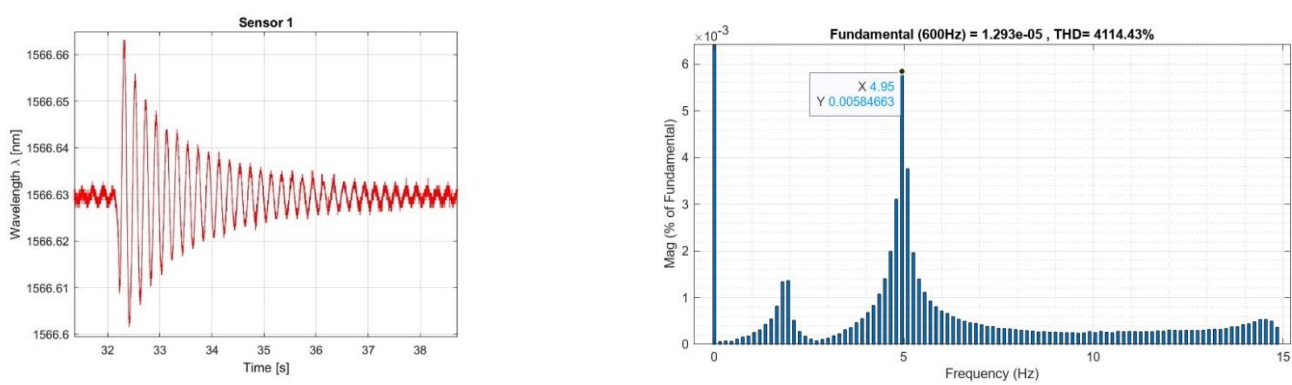


Figure 11 – FBG response (left) and FFT analysis (right)

3.3 Flight test

After completing the ground tests, the entire architecture was also tested in flight. In this case, the deformations measured by the FBG sensors are caused by the aerodynamic loads induced by the maneuvers performed by the pilot. The data collected during the testing phase, which included repeating different flights, each lasting several minutes, confirm the high sensitivity and immediate responsiveness of the FBG sensors, as already verified with the measurements carried out on the ground. In particular, by analyzing the overall trend provided by all the sensors placed on the same wing, it is possible to distinguish the different peaks caused by the turns imposed by the pilot. Furthermore, considering the different amplitudes of these peaks, it is possible to verify and reconstruct the distribution of the sensors along the wingspan.

A preliminary comparison between the trend provided by each FBG and the acceleration measured along the aircraft's z-axis also highlights the consistency between the two measurements. However, during the first flight test phase, the telemetry system could not completely satisfy the requirement of 10 Hz, while the onboard IMU worked at 200 Hz. Consequently, the highly significant difference in the two sampling frequencies still does not allow for a precise comparison of the two curves.

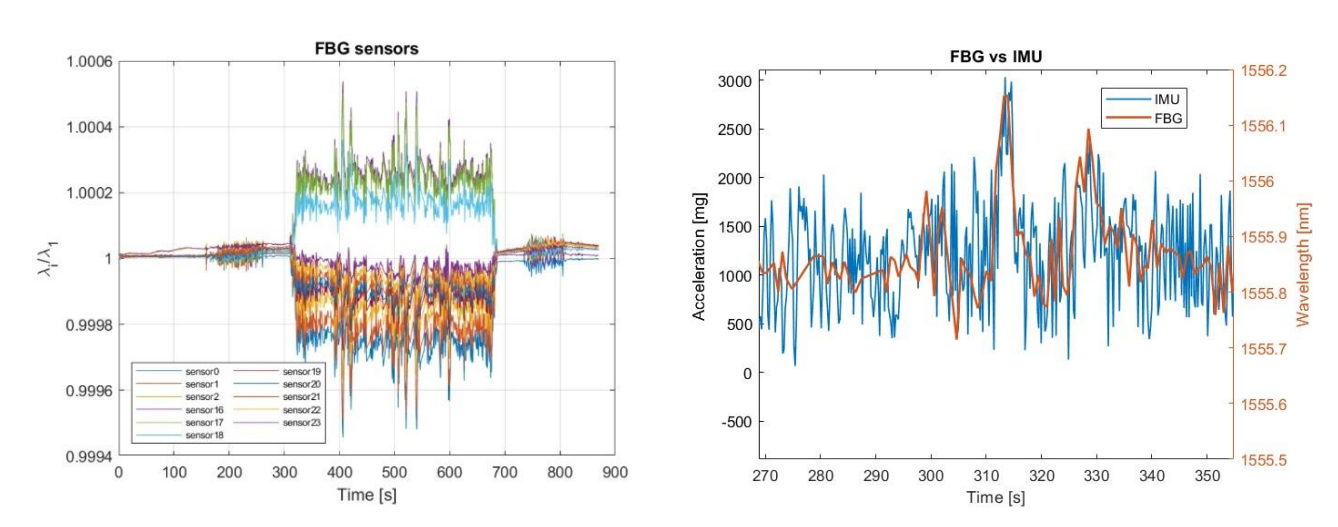


Figure 12 – Overall FBG fligth test data (left) and comparison FBG-IMU (right)

The great sensitivity and extreme speed in response by FBG sensors is also easy to understand by going into more detail on the data shown in the figure 11. The trends can be categorized into four phases delineated by different level of oscillations: initial fiber activation, Anubi transportation to the runway, maneuvering phases, and landing. Initially, spanning from 0 to 172 seconds, is the phase of initial fiber activation, where the increasing wavelength values correspond to the temperature rise in the fibers.

Subsequently, from 172 to 216 seconds, Anubi's transfer from the canopy to the runway is marked by oscillations detected by the sensors, indicative of this movement. It is noteworthy that all sensors, except for 16, 17, and 18, are positioned on the upper face of the wing. This is evidenced by a ratio greater than 1, attributed to the weight of half the wing, affecting the longitudinal balance during the stationary phase. Following the take-off phase, a sequence of maneuvers ensues, characterized by significant wavelength oscillations. Notably, sensors 16, 17, and 18 exhibit a ratio greater than 1 in this phase, as they are subjected to traction due to the lift acting upon them, while the ratios for the remaining sensors are less than 1, indicating compression of the wing. So, once the data from the IMU and FBGs were visualized (sensor 18 was used in this case because the findings for the sensors positioned on the bottom of the wing are the same), they were compared in these plots to determine if they were consistent.

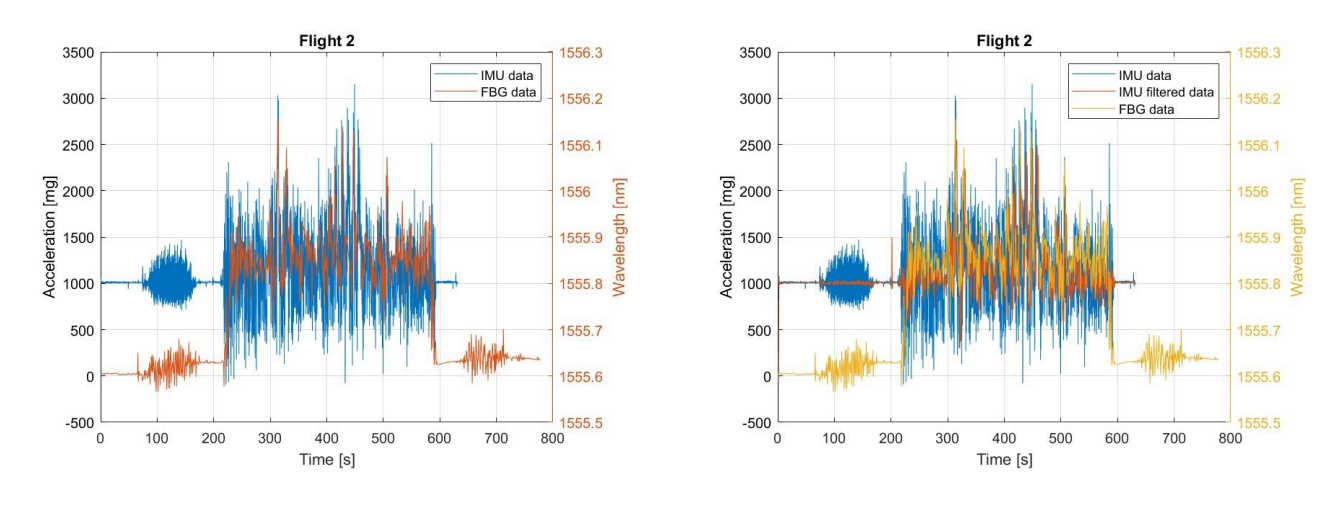


Figure 13 - Comparison between FBG and IMU data

The oscillations observed by the IMU unit appear to be larger than those detected by the FBG, necessitating the use of a Simulink-based low-pass filter. A low-pass filter (LPF) is a circuit that only allows signals below its cutoff frequency while reducing any frequencies above it. It is the opposite of a high-pass filter, which only allows signals above its cutoff frequency and rejects all signals below it. For this filter, the Stopband edge frequency was set to 1.52 Hz, which was the acquisition frequency in flight imposed on the SOC, therefore frequencies greater than that value were shut off, while lower frequencies were passed through and shown.

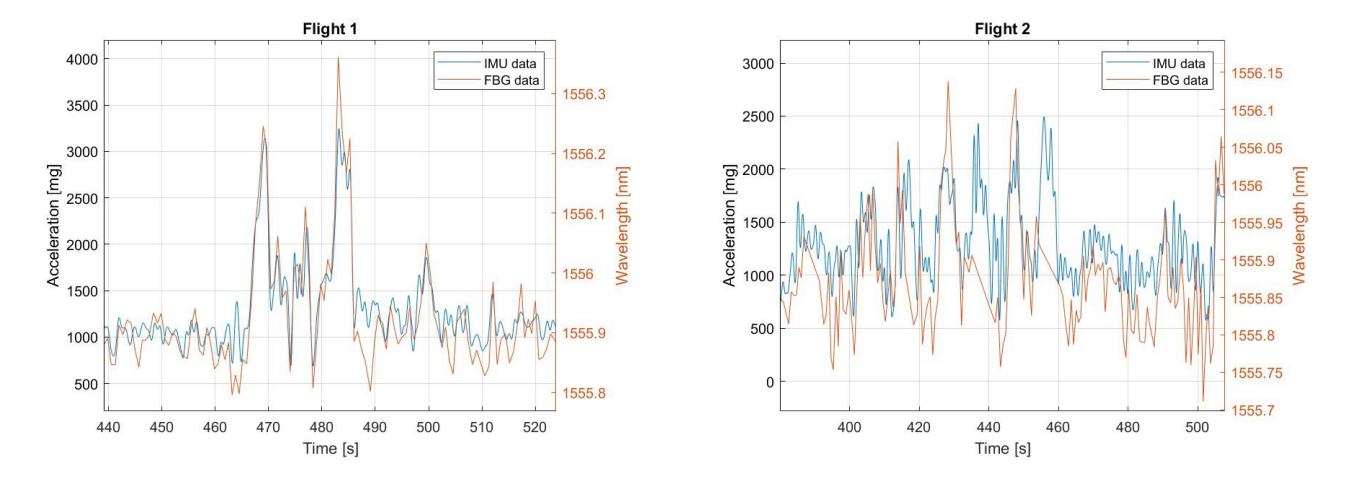


Figure 14 - Comparison between FBG and IMU data

4. Conclusions and Future development

The FBG-based sensors demonstrate their efficacy in capturing dynamic structural changes during maneuvers, offering valuable insights into both mechanical deformation and temperature fluctuations. Comparing the results provided by the FBG network with the data supplied by a traditional accelerometer placed on the UAV throughout all phases, the proposed system presents a promising approach to provide an alternative data source, thereby enhancing the reliability of current navigation systems. This sensor network, therefore, enables the provision of a dataset originating from a distinct physical principle, consequently avoiding the same sources of disturbance and malfunction. This preliminary results represent a fundamental step in order to achieve future goal of the project, in particular by developing a robust FBG's data control logic and a more powerful telemetry system.

5. Contact Author Email Address

The contact author is: alessandro.aimasso@polito.it

6. Copyright Statement

The authors confirm that they, and/or their company or organization, hold copyright on all of the original material included in this paper. The authors also confirm that they have obtained permission, from the copyright holder of any third party material included in this paper, to publish it as part of their paper. The authors confirm that they give permission, or have obtained permission from the copyright holder of this paper, for the publication and distribution of this paper as part of the ICAS proceedings or as individual off-prints from the proceedings.

References

- [1] Safa, Kasap. Optoelectronics and photonics: principles and practices. Prentice Hall, 2001.
- [2] G P Agrawal and S. Radic. Phase-Shifted Fiber Bragg Gratings and their Application for Wavelength Demultiplexing. *IEEE Photonics Technology Letters*, vol. 6, no. 8, pp. 995–997, 1994.
- [3] S J. Mihailov et al. Extreme Environment Sensing Using Femtosecond Laser-Inscribed Fiber Bragg Gratings.
- [4] S J Mihailov. Fiber Bragg Grating Sensors for Harsh Environments. *Sensors*, vol. 12, pp. 1898–1918, 2012.
- [5] S J Mihailov *et al*. Ultrafast laser processing of optical fibers for sensing applications. *Sensors*, vol. 21, no. 4. MDPI AG, pp. 1–23, Feb. 02, 2021.
- [6] R Rodríguez-Garrido *et al.* High-temperature monitoring in central receiver concentrating solar power plants with femtosecond-laser inscribed fbg. *Sensors*, vol. 21, no. 11, Jun. 2021.
- [7] A Behbahani, M. Pakmehr, and W. A. Stange. Optical Communications and Sensing for Avionics," in *Springer Handbooks*, Springer Science and Business Media Deutschland GmbH, 2020, pp. 1125–1150. doi: 10.1007/978-3-030-16250-4 36.
- [8] A C Marceddu *et al.*, "Air-To-Ground Transmission and Near Real-Time Visualization of FBG Sensor Data Via Cloud Database. *IEEE Sensor Journal*, 2022.
- [9] A Aimasso.. Optical fiber sensor fusion for aerospace systems lifecycle management. *Materials Research Proceedings*, 2023.
- [10] R Di Sante. Fibre optic sensors for structural health monitoring of aircraft composite structures: Recent advances and applications. *Sensors (Switzerland)*, vol. 15, no. 8, pp. 18666–18713, Jul. 2015.
- [11] E J Friebele *et al.* Optical fiber sensors for spacecraft applications, *Smart Mater. Struct*, vol. 8, pp. 813–838, 1999.
- [12] I McKenzie, S Ibrahim, E Haddad, S Abad, A Hurni, and L. K. Cheng. Fiber Optic Sensing in Spacecraft Engineering: An Historical Perspective From the European Space Agency. *Frontiers in Physics*, vol. 9. Frontiers Media S.A., Nov. 15, 2021.
- [13] A. Aimasso, M D L D Vedova, and P Maggiore. Sensitivity analysis of FBG sensors for detection of fast temperature change. *Journal of Physics: Conference Series*, 2023.
- [14] A. Aimasso, M D L Dalla Vedova, and P. Maggiore. Analysis of FBG Sensors Performances When Integrated Using Different Methods for Health and Structural Monitoring in Aerospace Applications. 2022 6th International Conference on System Reliability and Safety, ICSRS 2022, 2022.
- [15] C G Ferro, A Aimasso, M Bertone, N Sanzo, M D L D Vedova, and P Maggiore. Experimental development and evaluation of a fiber bragg grating-based outside air temperature sensor for aircraft applications. *Transportation Engineering*, vol. 14, 2023.